 doi:10.20944/preprints202208.0454.v1

Article

Spectroscopy Study of Isothermal Spin State Switching in a Fe (II) Spin Crossover Molecular Thin Film

Saeed Yazdani[1,*] Kourtney Collier[2], Grace Yang[3], Jared Phillips[1], Ashley Dale[1], Samuel Grocki[4], Jian Zhang[5], Ruihua Cheng[1,*] Peter A. Dowben[6,*]

[1] Department of Physics, Indiana University Purdue University Indianapolis (IUPUI), Indianapolis, IN 46202, USA; syazdani@iupui.edu (S.Y.); japphill@iu.edu (J.P.); daleas@iu.edu (A.D.); rucheng@iupui.edu (R.C.)
[2] Department of Mechanical and Energy Engineering, Purdue School of Engineering, Indianapolis, IN 46202, USA; kocollie@iu.edu (K.C)
[3] Carmel High School, Carmel, IN 46032 USA; gracewenyiyang@gmail.com (G.Y.)
[4] Department of Chemistry, Purdue University, West Lafayette, IN 47907, USA; sgrocki@purdue.edu (S.G.)
[5] Molecular Foundry, Lawrence Berkeley National Laboratory, Berkeley, CA 94720, USA; jianzhang@lbl.gov (J.Z.)
[6] Department of Physics and Astronomy, Jorgensen Hall, University of Nebraska, Lincoln, NE 68588-0299, USA; pdowben@unl.edu (P.D.)

* Correspondence: syazdani@iupui.edu, rucheng@iupui.edu, pdowben@unl.edu

Abstract: Using optical characterization, it is evident that the spin state of the spin crossover molecular complex [Fe{$H_2B(pz)_2$}$_2$(bipy)] (pz = tris (pyrazol-1-1y)-borohydride, bipy = 2,2′-bipyridine) depends on the ferroelectric polarization of an adjacent thin film of the polymer ferroelectric polyvinylidene fluoride-hexafluoropropylene (PVDF-HFP). The UV-Vis spectroscopy reveals that room temperature switching of [Fe{$H_2B(pz)_2$}$_2$(bipy)] molecules in bilayers of PVDF-HFP/[Fe{$H_2B(pz)_2$}$_2$(bipy)] as a function of ferroelectric polar polarization. The electric polarity dependence of bilayers of PVDF-HFP/[Fe{$H_2B(pz)_2$}$_2$(bipy)] shows a strong dependence on the thickness of the PVDF-HFP layer. The PVDF-HFP/[Fe{$H_2B(pz)_2$}$_2$(bipy)] interface may affect polarization retention in the PVDF-HFP thin film limit.

Keywords: spin crossover; Fe (II) complex; isothermal switching; spintronics; thin films; UV Vis spectroscopy

1. Introduction

Functional spin crossover (SCO) molecular complexes exhibiting spin transition by external stimulation such as light, temperature, electric field, and magnetic field [1-9], have great potential for a new generation of molecular-based devices [4,9,10-26]. In SCO molecular compounds, depending on the ligand field strength, the transition metal ion can adopt two different stable spin states called the low spin (LS) state and the high spin (HS) state and can be switched between these two states [1,2,8-10]. The transition from high spin to low spin state for many spin crossover complexes occurs at extremely low temperatures. To implement these molecular systems for device applications, it is crucial to tailor them for use at room temperature. A ferroelectric layer capable of changing the polarity of the electric polarization in the presence of an external electric field facilitates the switching of spin states in SCO molecules at room temperature. [Fe{$H_2B(pz)_2$}$_2$(bipy)] is an SCO molecule that can be fabricated as a thin film via thermal evaporation in a high-vacuum atmosphere [14,15,27-32]. The transition temperature ($T_{1/2}$) and hysteresis of the spin state transition for [Fe{$H_2B(pz)_2$}$_2$(bipy)] thin films can vary depending on film thickness [31], however, even the highest possible $T_{1/2}$ value is still far below room temperature,

Preprints (www.preprints.org) | NOT PEER-REVIEWED | Posted: 26 August 2022 doi:10.20944/preprints202208.0454.v1

making it not practical for device applications. One method that can be utilized to facilitate and control the isothermal switching at room temperature between different spin states includes the use of a ferroelectric substrate of the deposited SCO molecules [11,14,15]. A polar interface, including a ferroelectric layer, can perturb the sublimated SCO molecules and influence the spin state transition [14,15,33,34]. PVDF is a piezoelectric polymer with ferroelectric characteristics [35,36]. Due to their unique properties, they are widely used in fabricating smart devices and sensors [37-45]. Yet sensing the ferroelectric polarization in a memory circuit is challenging and thus combining a ferroelectric with a SCO complex provides a facile mechanism for sensing and utilizing ferroelectric polarization in a nonvolatile device [11,14,15] because of the dramatic conductivity changes with spin state.

In this paper, the effect that ferroelectric PVDF-HFP film thickness and the polarity of electric polarization have on the switching behavior of $[Fe\{H_2B(pz)_2\}_2(bipy)]$ at room temperature is investigated. To achieve an optimal β phase in PVDF-HFP, thin films were annealed at different temperatures and characterized by Fourier-transform infrared (FTIR) spectroscopy. Switching to different spin states can lead to a change in the optical absorption spectrum [46]. UV-Vis spectroscopy was employed to study the temperature dependent spin state switching of a single layer of $[Fe\{H_2B(pz)_2\}_2(bipy)]$ and the isothermal switching of bilayer samples of PVDF-HFP/$[Fe\{H_2B(pz)_2\}_2(bipy)]$ with different PVDF-HFP thicknesses. The ability to detect the spin state by optical absorption measurements together with the ability to control the switching by external voltage makes the bilayer system an excellent candidate toward a potential next-generation molecular-based device.

2. Optical Characterization of the Spin State Change

A representative bond diagram of the $[Fe\{H_2B(pz)_2\}_2(bipy)]$ molecule is shown in figure 1 (a). The central Fe ion is bonded to nitrogen atoms from each of its ligands. N1 is the nitrogen of the bipyridine ligand while N2 and N3 correspond to the nitrogen atoms bonding the pyrazole ligands to the central Fe. The SCO transition for the $[Fe\{H_2B(pz)_2\}_2(bipy)]$ molecular compound depends upon the changes in the bond length and ligand angular orientation within the molecule [31,47]. When the molecule approaches the transition temperature, its bond lengths vary, and the ligands rotate. This change and rotation occur mainly between the Fe ion and the bipyridine ligand (Fe-N1 ligand) [31,47,48]. A longer bond length means a weaker interaction which tends to favor the HS state with a total spin $S = 2$, while a shorter bond length corresponds to a stronger interaction, leading to the LS state with a total spin $S = 0$.

Figure 1 (b) compares the infrared spectra of $[Fe\{H_2B(pz)_2\}_2(bipy)]$ in powder form with that of a thermally evaporated 300 nm thin film. A similar infrared spectrum for both bulk and thin film indicates a successful thermal sublimation without decomposition. The existence of B-H vibrations in both powder and thin film spectra at 2416 cm^{-1} and 2277 cm^{-1}, and C-H vibrations in 2841 cm^{-1}, 2911 cm^{-1}, and 3097 cm^{-1} verify that $[Fe\{H_2B(pz)_2\}_2(bipy)]$ molecules maintain their integrity after evaporation. Observing no significant changes in the IR spectra of powder and the thin film implies that similar thermal properties are expected [32]. Additionally, X-ray diffraction (XRD) patterns shown in Figure 1 (c) confirm that the thin film sample preserves the $[Fe\{H_2B(pz)_2\}_2(bipy)]$ crystalline structures however, the molecules of the thin film samples have certain preferential orientation on the substrate.

Preprints (www.preprints.org) | NOT PEER-REVIEWED | Posted: 26 August 2022 doi:10.20944/preprints202208.0454.v1

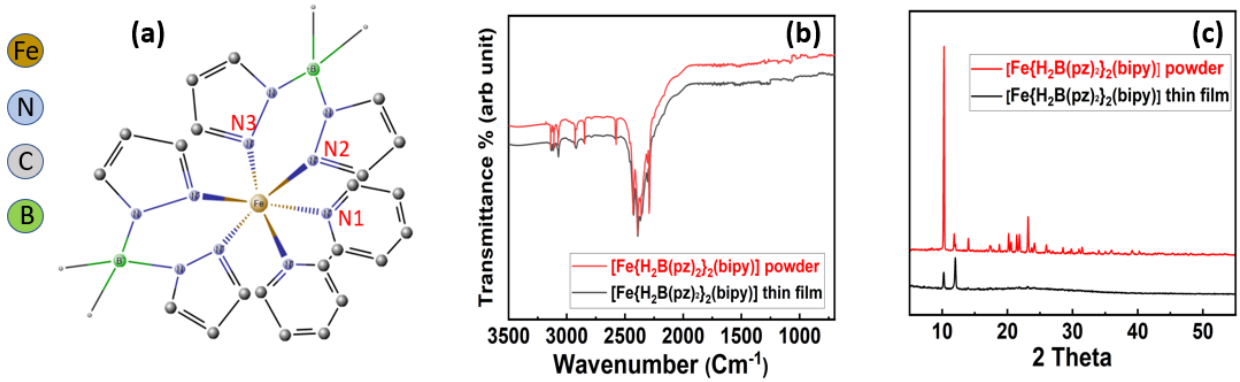

Figure 1. (a) The schematic diagram of [Fe{H2B(pz)2}2(bipy)] molecule. N1 is the nitrogen (blue) associated with the bipyridine ligand and N2 and N3 correspond to the nitrogen atoms in the pyrazole ligands. **(b)** The FTIR spectra of powder and 300 nm thin film [Fe{H2B(pz)2}2(bipy)] molecules. **(c)** The XRD patterns of [Fe{H2B(pz)2}2(bipy)] for powder and thin film samples respectively.

The spin transitions of the [Fe{H2B(pz)2}2(bipy)] thin films stimulated by thermal effects were measured using UV-Vis spectroscopy. Figure 2 (a) shows the temperature-dependent optical absorption spectra of a [Fe{H2B(pz)2}2(bipy)] thin film with a thickness of 300 nm in a wide temperature range from room temperature to around 120 K. The spectra were normalized for a better quantitative comparison between measurements at different temperatures. The optical absorption spectra of [Fe{H2B(pz)2}2(bipy)] molecules change with temperature and these changes can be associated with a change in spin state. In the HS state at room temperature, as a gentle peak in a wide range of wavelengths with a crest of around 530 nm was noticed. At the lower temperatures, spectral absorption intensity is dominated by two broad absorption bands centered at 410 nm, 570 nm, and 640 nm which is much more intense at lower temperatures corresponding to the LS than at the higher temperatures associated with the HS state. With decreasing temperature, these features in the UV-Vis spectra at around 410 nm, as well as 570 nm and 630 nm, gain significant intensity at about 173 K to 148 K, in the region of the spin state transition temperature of 160 K expected for evaporated thin films [32,49,50] and are fully realized by 133 K, a temperature associated with the LS state.

Figure 2 (b) is the UV-Vis spectra of the same thin film while increasing temperature of the of [Fe{H2B(pz)2}2(bipy)] thin film from low temperature to higher temperatures. The absorption spectra indicate that by increasing the temperature the molecules transition into the HS state from the LS state. At 148 K, peaks in the UV-VIS spectra at 410 nm, 570 nm, and 630 nm, are evident and are associated with the LS state of [Fe{H2B(pz)2}2(bipy)]. By increasing the temperature to 163 K, these sharp peaks in the UV-VIS spectra diminish, indicating the fractional transition of [Fe{H2B(pz)2}2(bipy)] molecules to the HS state. By increasing the temperature, the absorption spectra decreased as expected opposite to the previous behavior where the temperature was decreasing. The sharp peak at 410 nm disappears with increasing temperature but along with the features at 570 nm and 630 nm persist to 213 K. The much weaker feature at 530 nm is evident at 213 K and higher temperatures and is indicative of molecules are in the HS state. Although there is clearly some hysteresis in temperature, the very similar absorption spectrum as figure 2 (a) at 273 K in figure 2 (b), which differs significantly from the spectrum taken at 123 K (in figure 2 (a)) indicates the state switching of [Fe{H2B(pz)2}2(bipy)] is reversible and the [Fe{H2B(pz)2}2(bipy)] was successfully switched back to the HS state by increasing temperature.

By analyzing the absorption spectra at the same wavelength and different temperatures, the HS fraction of the [Fe{H2B(pz)2}2(bipy)] thin film at different temperatures was estimated. Figure 2 (c) shows the fraction of molecules in the HS state for thin films of [Fe{H2B(pz)2}2(bipy)] as a function of temperature. The calculated HS state fraction, with

Preprints (www.preprints.org) | NOT PEER-REVIEWED | Posted: 26 August 2022 doi:10.20944/preprints202208.0454.v1

temperature, indicates a transition temperature, ($T_{1/2}$), from the HS state to the LS state occurring around 160 K. This spin state transition temperature is in agreement with expectations from magnetic susceptibility for [Fe($H_2B(pz)_2)_2$(bipy)], agrees with other magnetic susceptibility data [32,47-51], as well as Mössbauer spectroscopy [48] and calorimetric measurements [48] (where $T_{1/2}$ = 159.5 K).

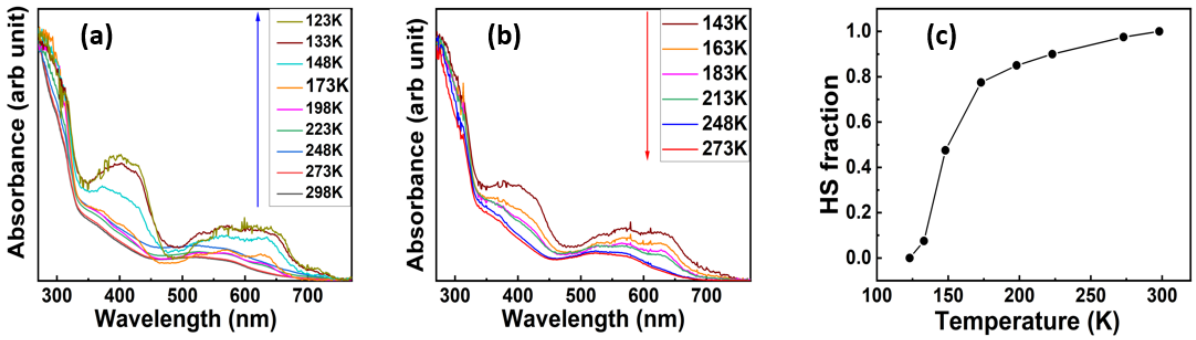

Figure 2. The temperature-dependent UV-Vis spectra of [Fe{$H_2B(pz)_2$}$_2$(bipy)] molecular thin film **(a)** from room temperature to low temperatures and **(b)** from low temperatures to room temperature. **(c)** The high spin (HS) state fraction of [Fe{$H_2B(pz)_2$}$_2$(bipy)] thin film as a function of temperature.

3. Molecular Ferroelectric Film Thickness Dependence

Voltage controlled nonvolatile switching of [Fe{$H_2B(pz)_2$}$_2$(bipy)] can be achieved well away from the thermal transition temperature (i.e., at room temperature), by combining a [Fe{$H_2B(pz)_2$}$_2$(bipy)] thin film with an organic ferroelectric, like PVDF-HFP [11,14,15]. To explore this further, we fabricated bilayer samples PVDF-HFP/[Fe{$H_2B(pz)_2$}$_2$(bipy)] to facilitate the isothermal switching at room temperature, by altering the electric polarization polarity of the PVDF-HFP thin film. The interface of SCO molecules can perturb the SCO functionality [9,28,29,52-54], and the effect of a ferroelectric is particularly profound [14,15,33,34,55]. The PVDF-HFP thin films tend to be mostly in the nonpolar α phase, when fabricated at room temperature, whereas the β phase is desirable due to its high boundary polarization. There are several approaches to achieving a dominant ferroelectric β phase (figure 3 (a)) in PVDF. One method is to use additives such as hydrated ionic salts, clay, PMMA, ZnO, TiO_2, and graphene [56,57]. In our case, however, a heat treatment method is preferred. It has been shown and repeatedly confirmed that one of the optimized ways to achieve the ferroelectric β phase crystalline ordering in PVDF-HFP thin films is thermal annealing [58-61]. A series of 150 layer thick PVDF-HFP samples were annealed at different temperatures (from 120-150 ◦C) for 180 minutes in an argon atmosphere changing the morphology of the PVDF-HFP thin films, as seen in the IR spectra of figure 3 (b).

While for thicker PVDF films, in the range of microns, X-ray diffraction (XRD) is a powerful tool for characterizing the crystalline structure, for PVDF-HFP thin films in the range of nanometer, XRD collects a very weak signal of the thin film. As here we are investigating much thinner films, our approach to the characterization of the different crystalline phases of the PVDF-HFP thin films is to use Fourier-transform infrared spectroscopy (FTIR). The IR bands at 841 cm^{-1} and 879 cm^{-1} correspond to the β phase. Before annealing a PVDF-HFP thin film, only a very weak signal of β-phase is detected, based on the data shown in figure 3 (b). The IR signature of the PVDF β-phase improves with annealing as indicated by the increase in the β-phase IR features. Clearly, annealing significantly improves the β-phase of the PVDF-HFP thin films.

Preprints (www.preprints.org) | NOT PEER-REVIEWED | Posted: 26 August 2022 doi:10.20944/preprints202208.0454.v1

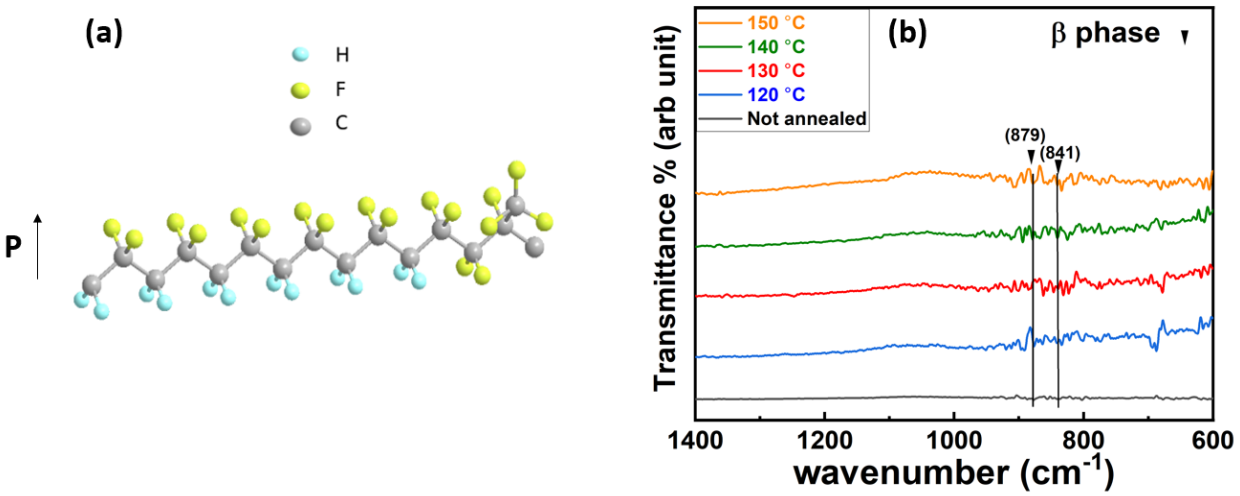

Figure 3. **(a)** A schematic diagram of PVDF-HFP in the β phase. **(b)** The FTIR spectroscopy of 150 layer thick PVDF-HFP thin films annealed at argon atmosphere for 180 minutes.

Decreasing the ferroelectric thin film thickness will decrease the coercive voltage [11,36], but for a nonvolatile device application there must be polarization retention [11]. To study the effect of PVDF-HFP polarization and thickness on isothermal switching of [Fe{$H_2B(pz)_2$}$_2$(bipy)] thin films, a series of samples with different layers of PVDF-HFP, ranging from 5 to 25 layers, with a constant thickness (300 nm) of [Fe{$H_2B(pz)_2$}$_2$(bipy)] were prepared (figures 4 (a) and 4 (b)). Sample preparation will be comprehensively explained in the materials and methods section later.

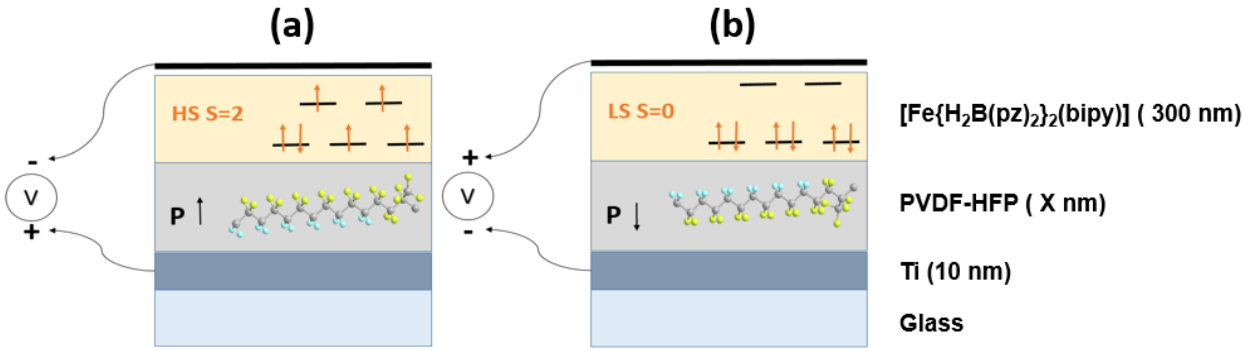

Figure 4. A schematic cross-section diagram of bilayer the PVDF-HFP/[Fe{$H_2B(pz)_2$}$_2$(bipy)] studied, with the polarization of PVDF-HFP thin film toward a specific direction can cause the upper SCO layer to switch to the **(a)** high spin (HS) or **(b)** low spin (LS) states schematically indicated.

Figure 5 (a) is the UV-Vis spectra of the bilayer sample with 5 monolayers PVDF-HFP with altered polarities at room temperature. Measurements show that for the sample with 5 layers of PVDF-HFP, isothermal voltage-controlled switching between the [Fe{$H_2B(pz)_2$}$_2$(bipy)] spin states do not occur by changing the electric applied to the adjacent PVDF-HFP thin film. Either the voltage applied was not high enough to overcome the coercive force of the PVDF-HFP layer, so the polarization was not altered, or the polarization prefers one direction (i.e., up) and polarization in the opposite direction (down) is not retained and quickly reverts to the favored polarization direction. This lack of polarization retention is a common problem with ferroelectric thin films, in the thin film limit [62,63]. In the absence of polarization retention, an "up" ferroelectric polarization as seen here is expected [64].

Preprints (www.preprints.org) | NOT PEER-REVIEWED | Posted: 26 August 2022 doi:10.20944/preprints202208.0454.v1

By increasing the thickness PVDF-HFP of the thin film to 15 layers, there is a coexistence of both the HS and the LS spin state in the adjacent [Fe{$H_2B(pz)_2$}$_2$(bipy)] layer, even before polarization, as seen in figure 5 (b). In terms of changing the spin state of the [Fe{$H_2B(pz)_2$}$_2$(bipy)] in the [Fe{$H_2B(pz)_2$}$_2$(bipy)] and PVDF-HFP bilayer structure, the best result was achieved for the sample fabricated with 25 layers of PVDF-HFP (figure 5 (c)). Reversible voltage-controlled switching from both the HS and the LS states of [Fe{$H_2B(pz)_2$}$_2$(bipy)] was observed and associated with the changing the polarity of the PVDF-HFP thin films. Before polarizing the PVDF-HFP layer, the optical absorption features associated with the LS state (410 nm) and HS state (530 nm) of [Fe{$H_2B(pz)_2$}$_2$(bipy)] (as discussed above) were not evident. By polarizing the PVDF-HFP upwards, the [Fe{$H_2B(pz)_2$}$_2$(bipy)] HS optical absorption peak at 530 nm was observed. On the other hand, [Fe{$H_2B(pz)_2$}$_2$(bipy)] molecules successfully switched to the LS state when the PVDF-HFP layers were polarized downward. These results agree with previous experiments, where the spin state and consequently the conductivity of [Fe{$H_2B(pz)_2$}$_2$(bipy)] molecules changed by altering the electric polarization direction of the adjacent PVDF-HFP thin films [14,15]. In other words, a thin layer of PVDF-HFP causes the [Fe{$H_2B(pz)_2$}$_2$(bipy)] molecules to become locked in their spin state due to the coercive force being dominant. However, a thicker PVDF-HFP layer not only causes a coexistence of both HS and LS states but also provides the ability to switch to different spin states by altering the polarity of the PVDF-HFP layer.

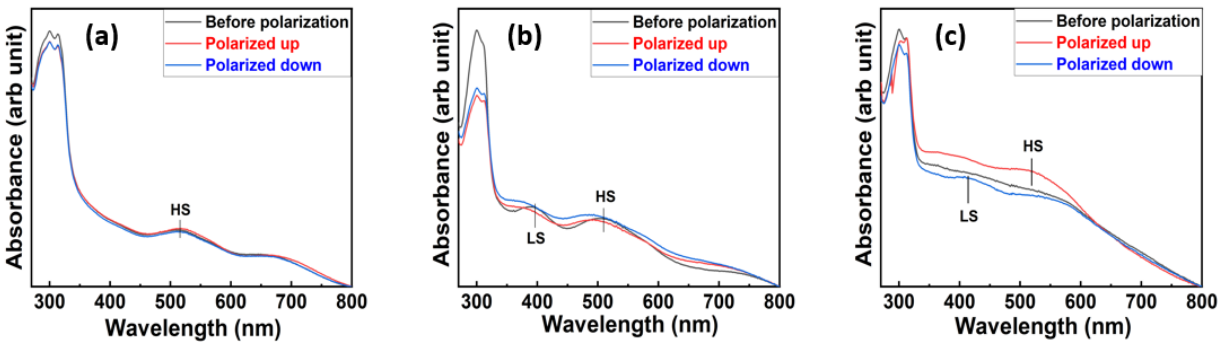

Figure 5. Room temperature UV-Vis spectra of the bilayer samples were made with **(a)** 5 layers **(b)** 15 layers and **(c)** 25 layers of PVDF-HFP substrates polarized toward different directions.

4. Materials and Methods

The [Fe{$H_2B(pz)_2$}$_2$(bipy)] molecules were synthesized as described in a previous article [49]. The method used to deposit the [Fe{$H_2B(pz)_2$}$_2$(bipy)] thin films was thermal evaporation under a high vacuum (10^{-8} Torr). Samples for temperature-dependent SCO transition studies were 300 nm [Fe{H_2B $(pz)_2$}$_2$(bipy)] thin films, thermally evaporated with an estimated growth rate of 0.2 nm/sec. Substrates were glass for the case of characterizing by UV-Vis and FTIR spectrometry. To study the effect of electric field on switching the spin state of [Fe{H_2B $(pz)_2$}$_2$(bipy)], bilayer PVDF-HFP/[Fe{H_2B $(pz)_2$}$_2$ (bipy)] thin films with different thicknesses of PVDF-HFP were fabricated. For bilayer samples, 10 nm of Ti was sputtered on the glass to act as the bottom electrode. Various thicknesses of PVDF-HFP were deposited using a lab-built Langmuir-Blodgett (LB) machine. PVDF-HFP in solution was suspended in a water sub-phase for layer-by-layer LB deposition. A solution of 0.05% by weight of PVDF-HFP in acetone was made by mixing a 40 mg PVDF-HFP pill with 100 mL acetone and then heating to 90°C until complete solvation was achieved. This solution was then added to de-ionized milli-Q water at 1.5 µL per square centimeter of surface area for monolayer coverage of the water's surface. Then, 380 µL of acetone solution was added to the LB machine reservoir. For these parameters, each dip provides a thickness of around 0.7 nm. Samples were annealed within a nitrogen environment for 3 hours at 140 °C, which lead to a desirable β phase creation in the PVDF-HFP layer. Samples were then transferred back to the high vacuum chamber receiving an

 doi:10.20944/preprints202208.0454.v1

additional 30 nm of [Fe{H_2B $(pz)_2\}_2$(bipy)] via evaporation. A lab-built poling device with a removable top electrode was used to polarize the PVDF-HFP layer for bilayer samples. Using silver paint, a gold wire was attached to the bottom electrode of Ti thin film and then connected to a DC power supply. The removable top electrode approached the surface of the thin film until it was remarkably close in micron scale. Then, depending on the desired polarity of the PVDF-HFP layer, a negative or positive voltage of 30 V was applied. After waiting at the maximum voltage (+/-30 V) for 1 minute the bias voltage was ramped back to zero.

5. Conclusion

In this paper, switching of the spin state for [Fe{$H_2B(pz)_2\}_2$(bipy)] SCO molecular thin films were studied by optical spectroscopy. Temperature dependent UV-Vis measurements confirmed that the transition temperature $T_{1/2}$ from the HS to LS spin state occurs at around 160 K, consistent with prior studies. FTIR spectroscopy of PVDF-HFP revealed that post-annealing treatments lead to an improvement in the β phase for PVDF-HFP thin films. A thin film of PVDF-HFP in the β phase can allow isothermal switching of the spin state of [Fe{$H_2B(pz)_2\}_2$(bipy)] thin films at room temperature. Yet polarization retention is a problem in ferroelectric PVDF-HFP spin crossover [Fe{$H_2B(pz)_2\}_2$(bipy)] bilayers, so choosing the correct thickness of PVDF-HFP is crucial. Our experiment indicates that switching different spin states [Fe{$H_2B(pz)_2\}_2$(bipy)], in a ferroelectric PVDF-HFP spin crossover [Fe{$H_2B(pz)_2\}_2$(bipy)] bilayer, is possible with 25 layers of PVDF-HFP which corresponds to a thickness of around 20 nm.

Author Contributions: Conceptualization: R.C., P.D.; methodology, R.C., S.Y.; formal analysis, S.Y., R.C., J.P., K.C., P.D.; Software, S.Y., K.C; investigation, S.Y., K.C., J.P., A.D., S.G., G.Y., J.Z.; original draft preparation, S.Y.; writing—review and editing, J.P, S.Y. R.C., and P.D.; supervision, R.C.; funding acquisition, P.D., R.C.; All authors have read and agreed to the published version of the manuscript."

Funding: This research was supported by the National Science Foundation through NSF-DMR 2003057.

Institutional Review Board Statement: Not applicable.

Informed Consent Statement: Not applicable.

Data Availability Statement: Not applicable

Conflicts of Interest: The authors declare no conflict of interest.

References

1. Halcrow, M.A.; The foundation of modern spin-crossover. *Chemical Communications*. **2013**, 49, 93, 10890-10892.
2. Collet, E.; Guionneau, P.; Structural analysis of spin-crossover materials: From molecules to materials. *Comptes Rendus Chimie*. **2018,** 21, 12, 1133-1151.
3. Thakur, S.; Golias, E.; Kumberg, I.; Kumar, K.S.; Hosseinifar, R.; Torres-Rodriguez, J.; Kipgen, L.; Lotze, C.; Arruda, L.M.; Luo, C.; Radu, F.; Ruben, M.; Kuch, W.; Thermal-and Light-Induced Spin crossover Characteristics of a Functional Iron (II) Complex at Submonolayer Coverage on HOPG. *The Journal of Physical Chemistry C*. **2021**, 125, no. 25, 13925-13932.
4. Mahfoud, T.; Molnár, G.; Bonhommeau, S.; Cobo, S.; Salmon, L.; Demont, P.; Tokoro, H.; Ohkoshi, S.; Boukheddaden, K.; and Bousseksou, A.; Electric-field-induced charge-transfer phase transition: A promising approach toward electrically switchable devices. *Journal of the American Chemical Society*. **2009**, 131, no. 41, 15049-15054.
5. Ridier, K.; Nicolazzi, W.; Salmon, L.; Molnár, G.; Bousseksou, A.; Sequential Activation of Molecular and Macroscopic Spin-State Switching within the Hysteretic Region Following Pulsed Light Excitation. *Advanced Materials*. **2022**, 34, no. 6, 2105468.
6. Xie, K.; Ruan, Z.; Chen, X.; Jiong Yang, Wu, S.; Ni, Z.; Tong, M.; Light-induced hidden multistability in a spin crossover metal–organic framework. *Inorganic Chemistry Frontiers.* **2022,** *9*, 8, 1770-1776
7. Terrero, R.; Avila, Y.; Mojica, R.; Cano, A.; Gonzalez, M.; Avila, M.; and Reguera, E.; Thermally induced spin-crossover in the Fe(3-ethynylpyridine)$_2$[M(CN)$_4$] series with M= Ni, Pd, and Pt. The role of the electron density found at the CN 5σ orbital. *New Journal of Chemistry*. **2022**, 46, 20, 9618-9628.

8. Gütlich, P.; Goodwin, H.A; Garcia, Y.; Spin crossover in transition metal compounds. *Springer Science & Business Media* **2004**, Vol. 1
9. Kumar, K.S.; Ruben, M.; Sublimable Spin-Crossover Complexes: From Spin-State Switching to Molecular Devices. *Angewandte Chemie International Edition*. **2021**, 60, 14, 7502-7521.
10. Gütlich, P.; Garcia, Y.; Goodwin, H.A.; Spin crossover phenomena in Fe (ii) complexes. *Chemical Society Reviews* **2000,** 29, 6, 419-427.
11. Ekanayaka, T.K.; Hao, G.; Mosey, A.; Dale, A.S.; Jiang, X.; Yost, A.J.; Sapkota, K.R.; Wang, G.T.; Zhang, J.; N'Diaye, A.T.; Marshall, A.; Cheng, R.; Naeemi, A.; Xu, X.; Dowben, P.A. Nonvolatile Voltage Controlled Molecular Spin-State Switching for Memory Applications. *Magnetochemistry*. **2021**, 7, 37. https://doi.org/10.3390/magnetochemistry7030037
12. Molnár, G.; Salmon, L.; Nicolazzi, W.; Terki, F.; Bousseksou, A.; Emerging properties and applications of spin crossover nanomaterials. *Journal of Materials Chemistry C* .**2014**, 2, no 8, 1360-1366.
13. Tissot, A.; Kesse, X.; Giannopoulou, S.; Stenger, I.; Binet, L.; Rivière, E.; Serre, C.; A spin crossover porous hybrid architecture for potential sensing applications. *Chemical Communications*. **2019**, 55, no. 2, 194-197.
14. Mosey, A.; Dale, A.S.; Hao, G.; N'Diaye, A.; Dowben, P.A.; Cheng, R.; Quantitative study of the energy changes in voltage-controlled spin crossover molecular thin films. *The Journal of Physical Chemistry Letters*. **2020**, 11, 9, 8231-8237.
15. Hao, G.; Mosey, A.; Jiang, X.; Yost, A.J.; Sapkota, K.R.; Wang, G.T.; Zhang, X.; Zhang, J.; N'Diaye, A.T.; Cheng, R.; Xu, X.; Non-volatile voltage controlled molecular spin state switching. *Applied Physics Letters*. **2019**, 114, 3, 032901.
16. Kahn, O.; Martinez, C. J. Spin-Transition Polymers: From Molecular Materials Toward Memory Devices. *Science* **1998**, *279*, 44-48, doi: 10.1126/science.279.5347.44.
17. Bousseksou, A.; Molnár, G.; Salmon, L.; Nicolazzi, W. Molecular Spin Crossover Phenomenon: Recent Achievements and Prospects. *Chem. Soc. Rev*. **2011**, *40*, 3313–3335, doi: 10.1039/c1cs15042a.
18. Bousseksou, A.; Molnár, G.; Demont, P.; Menegotto, J. Observation of a Thermal Hysteresis Loop in the Dielectric Constant of Spin Crossover Complexes: Towards Molecular Memory Devices. *J. Mater. Chem.* **2003**, *13*, 2069-2071, doi: 10.1039/B306638J.
19. Molnár, G.; Rat, S.; Salmon, L.; Nicolazzi, W.; Bousseksou, A. Spin Crossover Nanomaterials: From Fundamental Concepts to Devices. *Adv. Mater.* **2018**, *30*, 17003862, doi: 10.1002/adma.201703862.
20. Rotaru, A.; Dugay, J.; Tan, R. P.; Guralskiy, I. A.; Salmon, L.; Demont, P.; Carrey; J.; Molnár, G.; Respaud, M.; Bousseksou A. Nano-electromanipulation of Spin Crossover Nanorods: Towards Switchable Nanoelectronic Devices. *Adv. Mater.* **2013**, *25*, 1745–1749, doi: 10.1002/adma.201203020.
21. Lefter, C.; Davesne, V.; Salmon, L.; Molnár, G.; Demont, P.; Rotaru, A.; Bousseksou, A. Charge Transport and Electrical Properties of Spin Crossover Materials: Towards Nanoelectronic and Spintronic Devices. *Magnetochemistry*. **2016**, *2*,18, doi:10.3390/magnetochemistry2010018.
22. Lefter, C.; Tan, R.; Dugay, J.; Tricard, S.; Molnár, G.; Salmon, L.; Carrey, J.; Nicolazzi, W.; Rotaru, A.; Bousseksou, A. Unidirectional Electric Field-Induced Spin-State Switching in Spin Crossover Based Microelectronic Devices. *Chem. Phys. Lett.* **2016**, *644*, 138–141, doi: 10.1016/j.cplett.2015.11.036.
23. Mahfoud, T.; Molnár, G.; Cobo, S.; Salmon, L.; Thibault, C.; Vieu,C.; Demont, P.; Bousseksou A. Electrical Properties and Non-Volatile Memory Effect of the [Fe(HB(pz)$_3$)$_2$] Spin Crossover Complex Integrated in a Microelectrode Device. *Appl. Phys. Lett.* **2011**, *99*, 053307, doi:10.1063/1.3616147.
24. Hao, G.; Cheng, R.; Dowben, P. A. The Emergence of the Local Moment Molecular Spin Transistor, *J. Phys. Condens. Matter* **2020**, *32*, 234002, doi: 10.1088/1361-648X/ab74e4.
25. Khusniyarov, M. M. How to Switch Spin-Crossover Metal Complexes at Constant Room Temperature *Chem. Eur. J*. **2016**, *22*, 15178 – 15191, doi: 10.1002/chem.201601140.
26. Kumar, K.S.; and Ruben, M.; Emerging trends in spin crossover (SCO) based functional materials and devices. *Coordination Chemistry Reviews*, **2017**, 346, pp.176-205.
27. Hao, G.; N'Diaye, A.T.; Ekanayaka, T.K.; Dale, A.S.; Jiang, X.; Mishra, E.; Mellinger, C.; Yazdani, S.; Freeland, J.W.; Zhang, J.; Cheng, R.; Xu, X.; Dowben, P.A. Magnetic Field Perturbations to a Soft X-ray-Activated Fe (II) Molecular Spin State Transition. *Magnetochemistry*. **2021**, 7, 135. https://doi.org/10.3390/magnetochemistry7100135
28. Beniwal, S.; Zhang, X.; Mu, S.; Naim, A.; Rosa, P.; Chastanet, G.; Létard, J.F.; Liu, J.; Sterbinsky, G.E.; Arena, D.A.; Dowben, P.A.; Surface-induced spin state locking of the [Fe(H$_2$B(pz)$_2$)$_2$(bipy)] spin crossover complex. *Journal of Physics: Condensed Matter*, **2016**, 28, 20, p.206002.
29. Zhang, X.; Jiang, X.; Zhang, X.; Yin, Y.; Chen, X.; Hong, X.; Xu, X.; Dowben, P.A.; Indications of magnetic coupling effects in spin cross-over molecular thin films. *Chemical Communications*. **2018**, 54, 8, 944-947.
30. Kumar, K.S.; Studniarek, M.; Heinrich, B.; Arabski, J.; Schmerber, G.; Bowen, M.; Boukari, S.; Beaurepaire, E.; Dreiser, J.; Ruben, M.; Engineering On-Surface Spin Crossover: Spin-State Switching in a Self-Assembled Film of Vacuum-Sublimable Functional Molecule. *Advanced Material.*, **2018**, 30, 11, 1705416.
31. Jiang, X.; Hao, G.; Wang, X.; Mosey, A.; Zhang, X.; Yu, L.; Yost, A.J.; DiChiara, A.D.; Cheng, X.; Zhang, J.; Cheng, R.; Dowben, P.A.; Tunable spin-state bistability in a spin crossover molecular complex. *Journal of Physics: Condensed Matter*. **2019**, 31, 31, p.315401.

32. Zhang, X.; Palamarciuc, T. Rosa, P.; Létard, J.-F.; Wu, N.; Doudin, B.; Zhang, Z-Z. Wang, J.; Dowben, P. A.; The Electronic Structure of a Spin Crossover Molecular Adsorbate," *Journ. Physical Chemistry C.* **2012**, 116, 23291–23296
33. Wäckerlin, C.; Donati, F.; Singha, A.; Baltic, R.; Decurtins, S.; Liu, S.X.; Rusponi, S.; Dreiser, J.; Excited spin-state trapping in spin crossover complexes on ferroelectric substrates. *The Journal of Physical Chemistry C*. **2018**, 122, 15,8202-8208.
34. Angulo-Cervera, J.E.; Piedrahita-Bello, M.; Mathieu, F.; Leichle, T.; Nicu, L.; Salmon, L.; Molnár, G.; Bousseksou, A.; Investigation of the Effect of Spin Crossover on the Static and Dynamic Properties of MEMS Microcantilevers Coated with Nanocomposite Films of [Fe(Htrz)$_2$(trz)](BF$_4$)@P(VDF-TrFE). Magnetochemistry. **2021**, 7, 8, 114.
35. Lovinger A. J., in Developments in Crystalline Polymers Vol. 1 (Ed. D C Basset) (London: *Elsevier Applied Science*, **1982**)
36. Blinov, L. M.; Fridkin, V. M.; Palto, S. P.; Bune, A. V.; Dowben, P. A.; Ducharme, S.; Two-Dimensional Ferroelectrics, *Uspekhi Fizicheskikh Nauk* [Russian edition vol.] **2000,** 170, 247-262; *Physics Uspekhi* [English edition volume] **2000**, 43, 243-257
37. Xin, Y.; Sun, H.; Tian, H.; Guo, C.; Li, X.; Wang, S.; Wang, C.; The use of polyvinylidene fluoride (PVDF) films as sensors for vibration measurement: A brief review. *Ferroelectrics*. **2016,** 502, 1, 28-42.
38. Lin, B. and Giurgiutiu, V., Modeling and testing of PZT and PVDF piezoelectric wafer active sensors. *Smart Materials and Structures*. **2006**, 15, 4, 1085.
39. Wang, F.; Tanaka, M.; Chonan, S.; Development of a PVDF piezopolymer sensor for unconstrained in-sleep cardiorespiratory monitoring. *Journal of intelligent material systems and structures.* **2003**, 14, 3, 185-190.
40. Li, Q., Xing, J., Shang, D. and Wang, Y., 2019. A flow velocity measurement method based on a PVDF piezoelectric sensor. *Sensors*. **2019**, 19, 7, 1657.
41. Shirinov, A.V.; Schomburg, W.K.; Pressure sensor from a PVDF film. *Sensors and Actuators A: Physica.* **2008** 142, 1, 48-55.
42. Martins, P.; Lopes, A.C.; Lanceros-Mendez, S.; Electroactive phases of poly (vinylidene fluoride): Determination, processing and applications. *Progress in polymer science*. **2014**, 39, 4, 683-706.
43. Ruan, L.; Yao, X.; Chang, Y.; Zhou, L.; Qin, G.; Zhang, X.; Properties and applications of the β phase poly (vinylidene fluoride). *Polymers*. **2018**, 10, 3, 228.
44. Singh, H.H.; Singh, S.; Khare, N.; Enhanced β-phase in PVDF polymer nanocomposite and its application for nanogenerator. *Polymers for Advanced Technologies*. **2018**, 29, 1, 143-150.
45. Kalimuldina, G.; Turdakyn, N.; Abay, I.; Medeubayev, A.; Nurpeissova, A.; Adair, D; Bakenov, Z.; A review of piezoelectric PVDF film by electrospinning and its applications. *Sensors*. **2020**, 20, 18, 5214.
46. Naggert, H.; Bannwarth, A.; Chemnitz, S.; von Hofe, T.; Quandt, E.; Tuczek, F.; First observation of light-induced spin change in vacuum deposited thin films of iron spin crossover complexes. *Dalton Transactions*. **2011**, 40, 24, 6364-6366.
47. Real, J.A.; Muñoz, M.C.; Faus, J.;Solans, X.; Spin crossover in novel Dihydrobis (1-pyrazolyl) borate [H$_2$B(pz)$_2$]-containing Iron (II) complexes. Synthesis, X-ray structure, and magnetic properties of [FeL{H$_2$B(pz)$_2$}$_2$] (L= 1, 10-Phenanthroline and 2, 2 '-Bipyridine). *Inorganic chemistry*. **1997**, 36, 14, 3008-3013.
48. Moliner, N.; Salmon, L.; Capes, L.; Munoz, M.C.; Létard, J.F.; Bousseksou, A.; Tuchagues, J.P.; McGarvey, J.J.; Dennis, A.C.; Castro, M.; Burriel, R.; Thermal and optical switching of molecular spin states in the {[FeL[H$_2$B(pz)$_2$]$_2$} spin-crossover system (L= bpy, phen). *The Journal of Physical Chemistry B*. **2002**, 106, 16, 4276-4283.
49. Palamarciuc, T.; Oberg, J. C.; Hallak, F. E.; Hirjibehedin, C. F.; Serri, M.; Heutz, S.; Létard, J.-F.; Rosa, P.; Spin crossover materials evaporated under clean high vacuum and ultra-high vacuum conditions: from thin films to single molecules. *J. Mater. Chem.* **2012**, *22*, 9690
50. Pronschinske, A.; Bruce, R. C.; Lewis, G.; Chen, Y.; Calzolari, A.; Buongiorno-Nardelli, M.; Shultz, D. A.; You, W.; Dougherty, D. B.; Iron(II) spin crossover films on Au(111): scanning probe microscopy and photoelectron spectroscopy. *Chem. Commun.* **2013**, *49*, 10446
51. Zhang, X.; Mu, S.; Chastanet, G.; Daro, N.; Palamarciuc, T.; Rosa, P.; Létard, J.-F.; Liu, J.; Sterbinsky, G.E.; Arena, D.A.; Etrillard, C.; Complexities in the Molecular Spin Crossover Transition. *J. Phys. Chem. C* **2015**, 119, 16293–23302
52. Gruber, M.; Berndt, R. Spin-Crossover Complexes in Direct Contact with Surfaces. *Magnetochemistry.* **2020**, 6, 35. https://doi.org/10.3390/magnetochemistry6030035
53. Yazdani, S.; Phillips, J.; Ekanayaka, T.K; Dowben, P.; Cheng, R.; The influence of the substrate on the functionality of spin crossover molecular materials. *Materials Today* **2022**, (submitted).
54. Zhang, X.; Costa, P. S.; Hooper, J.; Miller, D. P.; T. N'Diaye, A.; Beniwal, S.; Jiang, X.; Yin, Y.; Rosa, P.; Routaboul, L.; Gonidec, M.; Poggini, L.; Braunstein, P.; Doudin, B.; Xu, X.; Enders, A.; Zurek, E.; Dowben, P. A.; Locking and Unlocking the Molecular Spin Cross-Over Transition, *Advanced Materials.* **2017,** 32, 1702257; doi: 10.1002/adma.201702257
55. Zhang, X.; Palamarciuc, T.; Létard, J.-F.; Rosa, P.; Lozada, E. V.; Torres, F.; Rosa, L. G.; Doudin, B.; Dowben, P. A.; Spin State of a Molecular Adsorbate driven by the ferroelectric substrate polarization, *ChemComm.* **2014**, 50, 2255; DOI: 10.1039/c3cc46892e
56. Zhang, X.; Lang, W.Z.; Xu, H.P.; Yan, X.; Guo, Y.J.; Chu, L.F.; Improved performances of PVDF/PFSA/O-MWNTs hollow fiber membranes and the synergism effects of two additives. *Journal of Membrane Science*. **2014**, 469, 458-470.
57. Mokhtari, F.; Shamshirsaz, M.; Latifi, M.; Asadi, S.; Comparative evaluation of piezoelectric response of electrospun PVDF (polyvinilydine fluoride) nanofiber with various additives for energy scavenging application. *The Journal of the Textile Institute*, **2017**, 108, 6, 906-914.

58. Mahdavi Varposhti, A.; Yousefzadeh, M.; Kowsari, E; Latifi; M.; Enhancement of β-Phase crystalline structure and piezoelectric properties of flexible PVDF/Ionic liquid surfactant composite nanofibers for potential application in sensing and self-powering. *Macromolecular Materials and Engineering*. **2020**, 305,3,1900796.
59. Park, J.H.; Kurra, N.; AlMadhoun, M.N.; Odeh, I.N.; Alshareef, H.N.; A two-step annealing process for enhancing the ferroelectric properties of poly (vinylidene fluoride)(PVDF) devices. *Journal of Materials Chemistry C* **2015**, 3(10), pp.2366-2370.
60. Kaur, S.; Kumar, A.; Sharma, A.L; Singh, D.P.; Influence of annealing on dielectric and polarization behavior of PVDF thick films. *Journal of Materials Science: Materials in Electronics*. **2017**, 28(12), 8391-8396.
61. Satthiyaraju, M.; Ramesh, T.; Effect of annealing treatment on PVDF nanofibers for mechanical energy harvesting applications. *Materials Research Express*. **2019**, 6, 10,105366.
62. Scott, J.; Araujo C.; Meadows H.; McMillan L.; Shawabkeh A.:Radiation effects on ferroelectric thin-film memories: Retention failure mechanisms. *Journal of applied physics.* **1989**, 66, 3, 1444-1453.
63. Gao P.; Nelson C.; Jokisaari J.; Zhang Y.; Baek S.; Bark C.; Wang E.; Liu Y.; Li J.; Eom C.; Pan X.; Direct observations of retention failure in ferroelectric memories. *Advanced Materials.* **2012**, 24, 8, 1106-1110.
64. Duan, C-g.; Sabiryanov, R. F.; Liu, J.; Mei, W. N.; Dowben, P. A.; Hardy, J. R; Theoretical study of the magnetic ordering in rare-earth compounds with face-centered-cubic structure, *Journal of Applied Physics.* **2005,** 97, 10A915